Epidemic threshold and control in a dynamic network

Article (Published Version)

Epidemic threshold and control in a dynamic network

Michael Taylor,[1,*] Timothy J. Taylor,[1,2] and Istvan Z. Kiss[1]

[1]*School of Mathematical and Physical Sciences, Department of Mathematics, University of Sussex, Brighton UK-BN1 9QH, England, United Kingdom*

[2]*Centre for Computational Neuroscience and Robotics, University of Sussex, Brighton UK-BN1 9QH, England, United Kingdom*

(Received 2 June 2011; revised manuscript received 22 November 2011; published 5 January 2012)

In this paper we present a model describing susceptible-infected-susceptible-type epidemics spreading on a dynamic contact network with random link activation and deletion where link activation can be locally constrained. We use and adapt an improved effective degree compartmental modeling framework recently proposed by Lindquist *et al.* [J. Math Biol. **62**, 143 (2010)] and Marceau *et al.* [Phys. Rev. E **82**, 036116 (2010)]. The resulting set of ordinary differential equations (ODEs) is solved numerically, and results are compared to those obtained using individual-based stochastic network simulation. We show that the ODEs display excellent agreement with simulation for the evolution of both the disease and the network and are able to accurately capture the epidemic threshold for a wide range of parameters. We also present an analytical R_0 calculation for the dynamic network model and show that, depending on the relative time scales of the network evolution and disease transmission, two limiting cases are recovered: (i) the static network case when network evolution is slow and (ii) homogeneous random mixing when the network evolution is rapid. We also use our threshold calculation to highlight the dangers of relying on local stability analysis when predicting epidemic outbreaks on evolving networks.

DOI: 10.1103/PhysRevE.85.016103 PACS number(s): 89.75.Hc, 87.19.X−

I. INTRODUCTION

The rise in the popularity and relevance of networks as a tool for modeling complex systems is well illustrated by the ever increasing body of research concerned with the spread of diseases within host populations exhibiting nontrivial contact structures [1,2]. Networks offer an intuitive and relatively simple modeling framework which enables us to relax the strong implicit assumptions of approaches based on more classical ordinary differential equations (ODE) and to account for complexities in the contact structure of the host population [3–7]. This approach has shown that epidemic thresholds not only depend upon the infectiousness of the pathogen, or even simply the mean number of contacts per individual, but also upon the exact structure of the host population [8,9]. In addition to its inherent theoretical value, this paradigm has immediate practical benefits, as the primary role of public health services is to put measures in place to bring diseases below their epidemic threshold. These measures depend heavily upon disrupting the transmission of a disease through vaccination and also more directly through the closure of public services, or even quarantine and curfews in extreme cases. Hence the knowledge of how the structure of the host population is contributing to the spread of a disease would help to increase the efficacy of any intervention [10].

Despite advances in both rigorous and nonrigorous analysis of networks, a key assumption in many network models is that contacts are fixed for the duration of an epidemic and that the disease propagates with a constant intensity across links. This will not be true for many diseases, especially those with long infectious periods, or diseases that become endemic. Indeed, human contact patterns are well described by short repeated events, with individuals having a number of contacts best described by some appropriate time-dependent random variable [11]. Furthermore, individuals and the communities they belong to are likely to change their contact behavior as a result of natural evolution and endogenous or exogenous perturbations such as a disease outbreak [12].

Recently a number of studies have attempted to relax this assumption by allowing the networks to evolve over time by either varying contacts independently of the status of individuals [13,14] or by explicitly coupling contact activation and deletion to the disease status of individuals [15–17]. Thus, in the latter case, the dynamics of the disease is coupled with the dynamics of the network itself, with both acting as a feedback mechanism for the other [16,18,19]. Many of these studies have built macro-ODE-based models that describe the coevolution of networks and the diseases that spread along them [15–17,20]. All these studies confirm that dynamic networks and the coupling between the two dynamics lead to a richer spectrum of behavior than is found for epidemics on static networks.

A crucial feature of allowing the coevolution of disease and network is the interplay and feedback between both dynamics; however, this interdependence is difficult to measure empirically. The models developed so far mainly use rewiring rules that intuitively make sense given that individuals would have knowledge of the disease states of the rest of the population. However, in this paper we move away from these assumptions and we propose a dynamic network model that is based on random link activation-deletion, which would be more relevant for asymptomatic diseases, such as Chlamydia [21]. Furthermore, our dynamic network model is refined by introducing a local constraint on link activation to account for the difference in the magnitude of the number of contacts of a node relative to system size. This dynamic network coupled with the simple susceptible-infected-susceptible (SIS)

*mt264@sussex.ac.uk

disease dynamics leads to the full model that will be analyzed and discussed. We study this system and explore to what extent a macro-ODE-based compartmental model proposed for static networks is flexible enough to be adapted to a dynamic network case. Specifically, we focus on the SIS effective degree model as described in detail by Lindquist *et al.* [22] and also, to our knowledge, proposed by Marceau *et al.* [17] in close succession. Gleeson [23] later uses this same modeling framework and demonstrates that the effective degree formulation can be used to model other binary-state dynamics, such as Glauber spin dynamics, and shows that the ODE model can be used to carry out linear-stability-type analysis.

Whereas both Lindquist *et al.* [22] and Gleeson [23] confine themselves to modeling on static contact networks, Marceau *et al.* [17] uses this same improved effective degree formalism to explore SIS disease dynamics on adaptive networks. In this model the number of links in the network is fixed but the susceptible individuals can replace links to infectious neighbours with links to other randomly chosen susceptible individuals, as originally proposed by Gross *et al.* [15]. Our proposed model also uses SIS type epidemics on dynamic networks, but unlike Marceau our model allows for the random activation and deletion of links over time. As such, not only the network topology will evolve and change over time but also the number of links. This modified dynamic effective degree model is also governed by a closed set of ODEs, which is then solved and compared to results from individual-based simulations, and its ability to accurately predict the epidemic threshold over a range of parameters is investigated. We also derive an analytical R_0 calculation that describes the stability of the disease-free equilibrium, and we discuss the limitations of such a calculation in the light of having a dynamically active and evolving contact network.

II. THE MODEL

Linquist *et al.* [22] and Marceau *et al.* [17] use different notation to describe the same modeling framework. For consistency, in this paper we follow the notation used by the former throughout. The effective degree modeling approach for SIS-type disease dynamics [22] not only categorizes the disease state of each individual as susceptible (S) or infected (I) but also describes the state of their immediate neighborhood. This is achieved by keeping track of the number of susceptible and infected neighbors that belongs to a given node. For example, S_{si} represents the number of susceptible individuals that have s susceptible and i infected neighbours. This gives rise to more states and equations than would be seen in a standard pairwise model, where equations are given at the population level for all types of singles and pairs [24]. For example if a S_{si}-type node became infected via one of its i infectious neighbors, this individual would move to state I_{si} as only the status of the node itself is changing. However, if one of the i infected neighbors of an S_{si}-type node recovered then the node would enter the $S_{s+1,i-1}$ class, whereas infection of one of the s neighboring susceptible nodes moves the S_{si}-type node into the $S_{s-1,i+1}$ class.

Lindquist *et al.* [22] defined γ to be the per node recovery rate, β the per link infection rate, and M the maximum nodal degree of a network with N nodes. They then derived the following system of $\sum_{k=1}^{M} 2(k+1) = M(M+3)$ equations:

$$\dot{S_{si}} = -\beta i S_{si} + \gamma I_{si} + \gamma[(i+1)S_{s-1,i+1} - iS_{si}] + \beta \frac{\sum_{k=1}^{M}\sum_{j+l=k} jlS_{jl}}{\sum_{k=1}^{M}\sum_{j+l=k} jS_{jl}}[(s+1)S_{s+1,i-1} - sS_{si}], \quad (1)$$

$$\dot{I_{si}} = \beta i S_{si} - \gamma I_{si} + \gamma[(i+1)I_{s-1,i+1} - iI_{si}] + \beta \frac{\sum_{k=1}^{M}\sum_{j+l=k} l^2 S_{jl}}{\sum_{k=1}^{M}\sum_{j+l=k} jI_{jl}}[(s+1)I_{s+1,i-1} - sI_{si}], \quad (2)$$

for $\{(s,i) : s,i \geqslant 0, 1 \leqslant k = s+i \leqslant M\}$. This is the SIS effective degree model for a *static* contact network.

In order to adapt this model to describe SIS dynamics on a *dynamic* contact network, we introduce two new parameters: ω, the per link deletion rate; and α, the per nonlink, or more precisely the per *potential* link, creation rate. These rates could also be made to be link-type dependent; i.e., ω_{SI} would be the per SI link deletion rate. For the dynamic network case, the system size will increase slightly from $M(M+3)$ to $\sum_{k=0}^{M} 2(k+1) = (M+1)(M+2)$ equations to account for nodes of the type $X_{0,0}$ where $X \in \{S, I\}$. In the static case, these nodes were dynamically unimportant as they could neither infect nor become infected by other nodes. However, in the dynamic model, they could connect to other nodes in the system and so enter states $X_{1,0}$ or $X_{0,1}$ depending on the state of the node with which they have just formed a new link.

The total number of links in the system at time t, $\Lambda(t)$, and potential links, $\Phi(t)$, can easily be calculated from the effective degree formulation as

$$\Lambda(t) = \sum_{k=0}^{M}\sum_{j+l=k}(j+l)(S_{jl} + I_{jl}),$$

$$\Phi(t) = \sum_{k=0}^{M}\sum_{j+l=k}[M-(j+l)](S_{jl} + I_{jl}),$$

with the mean nodal degree given by $\langle k(t)\rangle = \frac{\Lambda(t)}{N}$. At the equilibrium, $\alpha\Phi = \omega\Lambda$, which gives us the mean nodal degree:

$$\langle k\rangle^* = \frac{\alpha}{\alpha+\omega}M. \quad (3)$$

Note that Eq. (3) does not depend on the system size, N, but rather on the maximum nodal degree, M. This is important because, in the static model, M is simply given by the node or nodes with the highest degree, while in the dynamic case, however, M can be considered as a carrying capacity, whereby no node can have more than M links. This subtle but important difference means that, in the dynamic case, M itself can be regarded as a parameter which controls the potential level of network saturation.

When adding the terms that govern link creation and deletion to Eqs. (1) and (2), it is far simpler to construct the terms that govern deletion of existing links than those for the creation of new links. Links to nodes of type X_{si} where $X \in \{S, I\}$ are cut at a rate proportional to their degree, so individuals will

leave X_{si} through link deletion at a rate $\omega(s+i)$ and will either enter the $X_{s-1,i}$ or $X_{s,i-1}$ classes depending on the state of the nodes to which they were previously connected. Similarly, individuals can enter state X_{si} if they were in states $X_{s,i+1}$ or $X_{s+1,i}$ and a link to an infected or susceptible node was deleted respectively.

When creating new links to nodes of type X_{si}, there are $M-(s+i)$ stubs remaining, so nodes will transition out of this state at a rate $\alpha[M-(s+i)]$ and will either enter the $X_{s+1,i}$ or $X_{s,i+1}$ classes depending on the state of the node to which they have just connected. The rate at which nodes enter the X_{si} class from either $X_{s-1,i}$ or $X_{s,i-1}$ depends not only on the number of stubs still available in the node in question, but also on the probability that the newly created link attaches to a node of state S or I, respectively. So nodes enter X_{si} from $X_{s-1,i}$ at the rate $\alpha P_S[M-(s-1+i)]$, and nodes enter X_{si} from $X_{s,i-1}$ at rate $\alpha P_I[M-(s+i-1)]$, where $P_X = \frac{\sum_{k=0}^{M}\sum_{j+l=k}[M-(j+l)]X_{jl}}{\sum_{k=0}^{M}\sum_{j+l=k}[M-(j+l)](S_{jl}+I_{jl})}, X \in \{S,I\}$ is the probability of picking an available stub belonging to nodes of type X where $X \in \{S,I\}$. The full set of transitions captured by this model is shown in Fig. 1.

The addition of these terms to Eqs. (1) and (2) transforms the SIS effective degree model for a static network into one that captures the spread of SIS-type diseases on a dynamic contact network and is described by the following system of

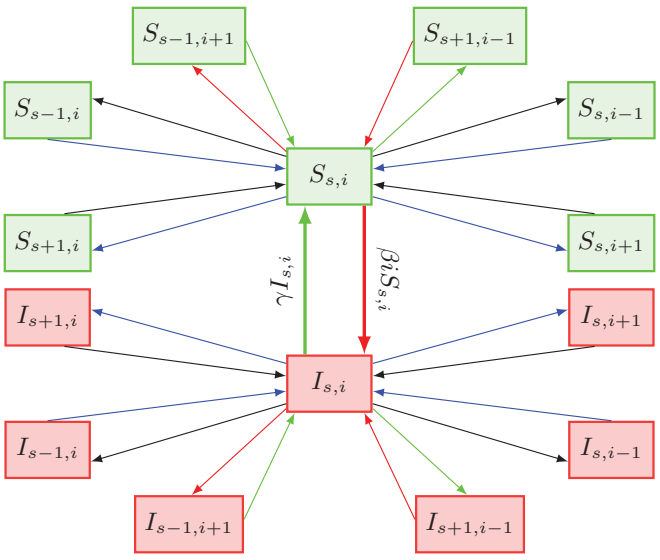

FIG. 1. (Color online) Flow chart showing transitions in the dynamic SIS effective degree model. The directed red (gray), green (light gray), blue (dark gray), and black lines represent changes in the state of an individual via infection, recovery, link creation, and link deletion, respectively. The thick lines represent changes to the individual, and thin lines represent changes to that individual's immediate neighborhood. In relation to nodes of type $X_{si}, X \in \{S,I\}$, infection of neighbors occurs at rate sG_X, recovery of neighbours at rate γi, creation of a susceptible (infectious) link at rate $\alpha[M-(s+i)]P_{S(I)}$, and deletion of a susceptible (infectious) link at rate $\omega s(i)$, where $G_S = \beta\frac{\sum_{k=1}^{M}\sum_{j+l=k} jlS_{jl}}{\sum_{k=1}^{M}\sum_{j+l=k} jS_{jl}}$, $G_I = \beta\frac{\sum_{k=1}^{M}\sum_{j+l=k} l^2S_{jl}}{\sum_{k=1}^{M}\sum_{j+l=k} jI_{jl}}$, and $P_X = \frac{\sum_{k=0}^{M}\sum_{j+l=k}[M-(j+l)]X_{jl}}{\sum_{k=0}^{M}\sum_{j+l=k}[M-(j+l)](S_{jl}+I_{jl})}$.

$(M+1)(M+2)$ equations:

$$\begin{aligned}\dot{S_{si}} &= -\beta i S_{si} + \gamma I_{si} + \gamma[(i+1)S_{s-1,i+1} - iS_{si}] \\ &+\beta\frac{\sum_{k=0}^{M}\sum_{j+l=k} jlS_{jl}}{\sum_{k=0}^{M}\sum_{j+l=k} jS_{jl}}[(s+1)S_{s+1,i-1} - sS_{si}] \\ &-\omega[(s+i)S_{si} - (i+1)S_{s,i+1} - (s+1)S_{s+1,i}] \\ &-\alpha[M-(s+i)]S_{si} + \alpha[M-(s-1+i)]P_S S_{s-1,i}, \\ &+\alpha[M-(s+i-1)]P_I S_{s,i-1}, \end{aligned} \tag{4}$$

$$\begin{aligned}\dot{I_{si}} &= \beta i S_{si} - \gamma I_{si} + \gamma[(i+1)I_{s-1,i+1} - iI_{si}] \\ &+\beta\frac{\sum_{k=1}^{M}\sum_{j+l=k} l^2S_{jl}}{\sum_{k=1}^{M}\sum_{j+l=k} jI_{jl}}[(s+1)I_{s+1,i-1} - sI_{si}] \\ &-\omega[(s+i)I_{si} - (i+1)I_{s,i+1} - (s+1)I_{s+1,i}] \\ &-\alpha[M-(s+i)]I_{si} + \alpha[M-(s-1+i)]P_S I_{s-1,i} \\ &+\alpha[M-(s+i-1)]P_I I_{s,i-1}, \end{aligned} \tag{5}$$

for $\{(s,i) : s,i \geqslant 0, 0 \leqslant k = s+i \leqslant M\}$. This system is the *dynamic* SIS effective degree model.

III. CALCULATING THE DISEASE THRESHOLD

For the static case, Lindquist *et al.* [22] used the next generation matrix approach [25] to calculate the disease threshold to be

$$\mathcal{R}_0 = \rho(FV^{-1}) = \frac{\beta}{\sum_{k=1}^{M} kS_{k,0}}\sum_{k=1}^{M} v_k^T V_k^{-1} u_k. \tag{6}$$

In this approach, Eqs. (4) and (5) are linearized at the disease-free equilibrium (DFE) and the Jacobian at the DFE is written as $F-V$. In this formulation, F accounts for transitions from disease-free states to disease states (in the static case, only the transition from $S_{s,0}$ to $S_{s-1,1}$ needs to be considered) and V accounts for transitions between different disease states. The spectral radius, ρ, the leading eigenvalue of FV^{-1}, gives R_0 and describes the stability of the DFE. If $R_0 < 1$ the DFE is stable and no epidemic will occur, but if $R_0 > 1$ the DFE is unstable and the infectious agent can spread through the population.

We can calculate F in the dynamic case by noting that the same $S_{s,0}$- to $S_{s-1,1}$-type transitions can still occur, but in addition nodes can enter the disease states by linking to an infected node, namely $S_{s,0}$ to $S_{s,1}$ transitions. If we introduce a subscript s to denote the static version of the next generation matrix, so the static version of F is called F_s and so on, we have

$$F_s = \frac{\beta}{\sum_{k=0}^{M} kS_{k,0}}\begin{bmatrix} u_{s_0} \\ u_{s_1} \\ \vdots \\ u_{s_M}\end{bmatrix}\begin{bmatrix} v_{s_0}^T v_{s_1}^T \dots v_{s_M}^T\end{bmatrix}, \tag{7}$$

where u_{s_k} and v_{s_k} are $(2k+1)$ x 1 vectors. The u_{s_k} vectors have $kS_{k,0}$ as their first entry and zeros elsewhere, and the v_{s_k} vectors have their first $(k-1)$ entries equal to $(k-1), 2(k-2), \dots, s(k-s), \dots, (k-1)$ and zeros elsewhere. This is almost identical to the F matrix constructed by Lindquist *et al.*,

but is augmented by u_{s_0} and v_{s_0} to account for the new disease state, $I_{0,0}$, and the summation starts at $k = 0$ rather than $k = 1$,

We now introduce a new subscript d to describe the new transitions that are only possible in the dynamic model. Hence a new F matrix, F_d, is created, which has exactly the same dimensions as F_s, and is given by

$$F_d = \frac{\alpha}{\sum_{k=0}^{M}(M-k)S_{k,0}} \begin{bmatrix} u_{d_0} \\ u_{d_1} \\ \vdots \\ u_{d_M} \end{bmatrix} \left[v_{d_0}^T v_{d_1}^T \dots v_{d_M}^T \right]. \quad (8)$$

Here, u_{d_k} is again a $(2k+1)$ x 1 vector with the first entry equal to $[M-(k-1)]S_{k-1,0}$ and all other entries equal to zero. In the case where $k = 0$, $u_{d_0} = (0)$. In addition, v_{d_k} is the same size as u_{d_k} and the first k entries are equal to zero, with the remaining $k+1$ entries equal to $M-k$. The final F matrix that captures all the possible transitions in the dynamic effective degree model is found by taking a linear sum of the two, namely $F = F_s + F_d$.

As with the static case, the V matrix is constructed through careful book-keeping, which can be done through iterative routines. In the static case, as the nodes have a fixed degree, V_s is a block-diagonal matrix with $V_s = V_{s_1} \oplus V_{s_2} \oplus \dots \oplus V_{s_M}$. For the dynamic model, V_d will be a block-tridiagonal matrix, as state transitions can now also occur by nodes gaining or losing a link. In addition, the extra disease state $I_{0,0}$ needs to be considered, and V will now also depend upon α and ω as well as β and γ. Once $F = F_s + F_d$ and $V = V_d$ are constructed, the leading eigenvalue or R_0 is computed numerically.

IV. RESULTS AND DISCUSSION

As shown in Fig. 2, the ODEs given by Eqs. (4) and (5) closely capture the time evolution of an epidemic as predicted by stochastic simulations. The only parameter that is varied in Fig. 2 is M, and it is interesting to note the effect it has on the evolution of the disease. As per Eq. (3), the mean nodal degree at equilibrium is dependent on M, and hence, given the same initial network configuration and values of α and ω, the network either loses or gains links as the system evolves. Thus varying the carrying capacity alone leads to different outcomes depending on whether the network can reach a level of connectedness that allows an epidemic to spread and become established. Allowing M to become an active model parameter that is able to control the outcome of an epidemic has potentially interesting real world implications. The number of contacts per person is a natural, countable property unlike the other model parameters, such as ω, which are more difficult to infer. Therefore local constraints that limit the maximum number of contacts per person could be potentially used as a metric when promoting safe behavior at a population level in the event of an outbreak or other public health crisis.

In Fig. 3, for a given value of α, M, and β, the epidemic threshold has been calculated from the ODEs in terms of ω and compared to that predicted by simulations. The agreement is excellent and this is strong evidence that the dynamic effective degree model accurately captures the evolution of an epidemic on a network with random link creation and deletion. When

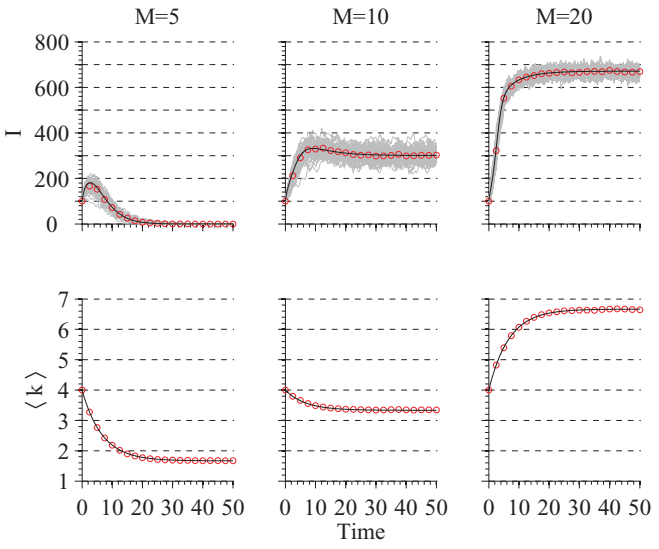

FIG. 2. (Color online) Time evolution of $I(t) = \sum_{k=0}^{M}\sum_{j+l=k} I_{jl}(t)$ and $\langle k\rangle(t) = \frac{\Lambda(t)}{N}$ for three different values of M. Results from the ODE are given by solid lines and those from simulation are given by points. In all cases, $N = 1000$, $I_0 = 100$, $\alpha = 0.05$, $\omega = 0.1$, $\beta = 0.5$, and $\gamma = 1$. The initial network is a regular random graph with $k = 4$. In each case, mean values from the stochastic simulations were found by averaging over 100 repetitions, with the individual realizations plotted in gray.

considering the (β,ω) parameter space used for the threshold plot in Fig. 3, there are three distinct regions that are worth noting. First, given an initial starting network, it is possible to calculate the threshold value of β in the static network case. For the regular random graph with $k = 4$ used here, that value is $\beta^* \approx 0.36$. For values of $\beta < 0.36$, the relative time scales of disease and network evolution are crucial in determining whether or not an epidemic will occur. In this situation, the network needs to quickly evolve to become more densely

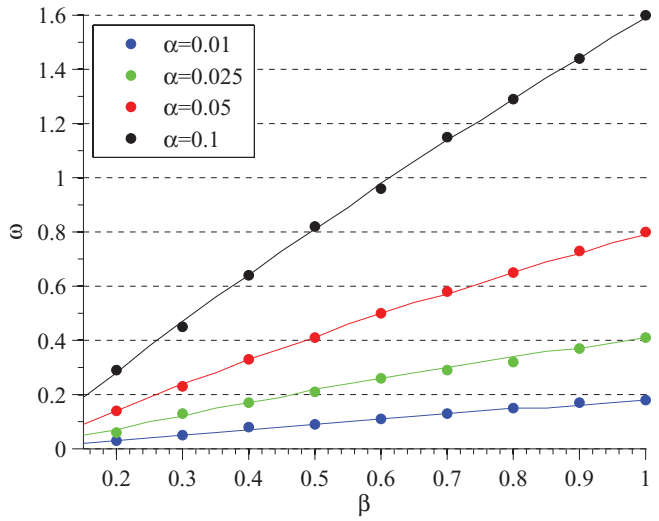

FIG. 3. (Color online) Epidemic threshold plot in the (β,ω) parameter space for four distinct values of α. Results from the ODE are given by solid lines and those from simulation are given by solid points. In each case, $N = 1000$, $I_0 = 10$, $M = 20$, and $\gamma = 1$. The initial network is a regular random graph with $k = 4$.

connected in order for there to be an outbreak. The second area of interest is when the disease is highly infectious and as a result requires a high value of ω to drive the epidemic below threshold. Indeed, if the disease parameters β and γ are fixed then the only way of affecting the outcome of an epidemic is through changing the network structure, i.e., reducing the number of links or the variance. Hence, for a fixed α and M, a value of β can be chosen large enough so that the minimum value of ω needed to reduce the connectivity of the network sufficiently to stop an outbreak (see Fig. 3) gives $\langle k\rangle^* < 2$, as can be calculated from Eq. (3). If a network has $\langle k\rangle^* < 2$ then it becomes fragmented, with many nodes becoming unconnected. In these situations, the value ω needed to prevent an epidemic virtually destroys the network. In terms of real world implications, a large value of ω could correspond to a situation of strict quarantine and curfew whereby links between individuals are kept to a minimum. In between these two cases lies a region within which an epidemic would take hold naturally, given the initial network, but which can be prevented by a value of ω that leaves the network well connected.

In Fig. 4, we show analytical values of R_0 for a range of values of β and α. It is worth noting that two limiting cases are recovered when the time scale of the network dynamics is fast and slow relative to the time scale of the disease dynamics. The thick short-dashed red line shows R_0 calculated for a static network, as proposed by Lindquist *et al.* [22] and given in Eq. (6), and this is exactly followed by results from our dynamic R_0 calculation when the network dynamics are set to be much slower than the disease dynamics. The other extreme is shown by the thick dash-dotted red line and

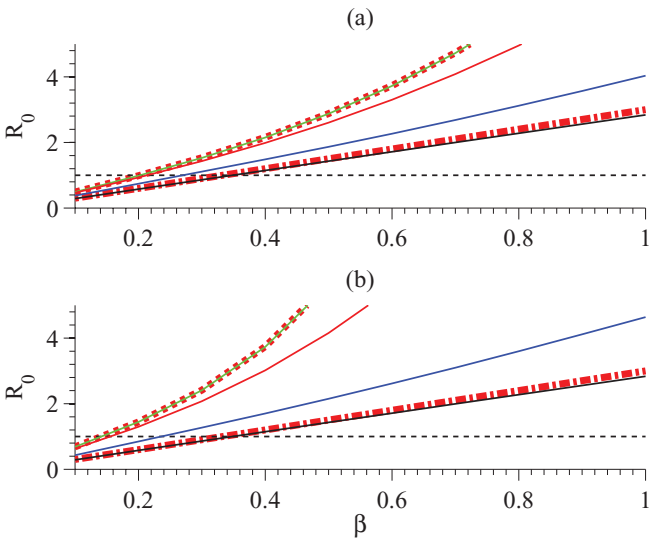

FIG. 4. (Color online) Threshold stability in the (β, R_0) space with $\gamma = 1$, $M = 20$, and $\langle k\rangle^* = 3$ for (thin solid lines, in order from top to bottom) $\alpha = 10^{-4}$ (green), $\alpha = 10^{-2}$ (red), $\alpha = 10^{-1}$ (blue), and $\alpha = 10$ (black). In (a) the initial network is a regular random graph with $k = 6$, and in (b) the initial degree distribution is a negative binomial with $\langle k\rangle = 6$ and $\sigma^2 = 12$. In each case, $\omega = \alpha\frac{M-\langle k\rangle^*}{\langle k\rangle^*}$. The thick short-dashed red line is the theoretical value of R_0 for a static network, and the thick red dash-dotted line is the mean-field limit $R_0 = \frac{\beta}{\gamma}\langle k\rangle^*$.

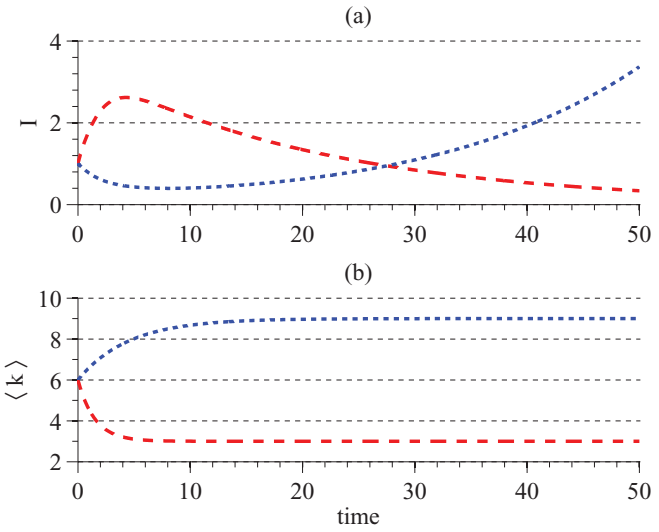

FIG. 5. (Color online) Time evolution of I and $\langle k\rangle$ with $\gamma = 1$, $M = 20$, $\alpha = 0.1$, $\omega = \alpha\frac{M-\langle k\rangle^*}{\langle k\rangle^*}$, and an initial regular random network with $k = 6$. The two cases illustrated above correspond to $\langle k\rangle^* = 3$ and $\beta = 0.35$, giving $R_0 \approx 1.29$ (red long-dashed line), and $\langle k\rangle^* = 9$ and $\beta = 0.125$, giving $R_0 \approx 0.77$ (blue short-dashed line).

is the value of R_0 that results from the classic mean-field calculation $R_0 = \frac{\langle k\rangle\beta}{\gamma}$. The time evolution of $\langle k\rangle$ is given by $\langle\dot{k}\rangle = \alpha(M - \langle k\rangle) - \omega\langle k\rangle$, but, when the network dynamics is fast, the equilibrium network distribution, and hence $\langle k\rangle^*$, is approached much quicker than the epidemic time scale, and hence a value of $\langle k\rangle = \langle k\rangle^*$ as given by Eq. (3) can be used. This limit is closely matched by results from our dynamic R_0 calculation when the network dynamics are rapid compared to disease transmission, as shown in Fig. 4.

Although Fig. 4 demonstrates the accuracy of our analytical R_0 calculation, Fig. 5 highlights two example cases where the long-term epidemic outcomes are the opposite of what is predicted by R_0. In the cases $R_0 < 1$ (blue short-dashed curve) and $R_0 > 1$ (red long-dashed curve), the system settles to an endemic and to a disease-free equilibrium, respectively, due to the different ways the networks evolve. Given that R_0 is based on a local stability analysis, it can only incorporate the immediate next generation effects of random link activation and deletion, and cannot account for long-term changes to the network structure. It is well established in the literature (see, for example Li *et al.* [26]) that R_0 is of limited value when used as a predictor, and even for static networks needs to be used with care. Our results add weight to this argument, and we show that when dealing with disease spreading through dynamic contact networks the use of R_0 as any kind of predictor on long-term disease evolution should be met with some degree of caution.

In summary, this paper has proposed an effective degree model for epidemics on dynamic networks with random link activation and deletion, where activation is locally constrained. We have shown that this model agrees extremely well with results obtained from stochastic simulations, and as such can reliably be used for the analytical and semianalytical study of coupled disease and network dynamics. We have shown how a local constraint limiting the number of contacts per

individual can be used to control and prevent the outbreak of an epidemic in this dynamic model. We have also proposed an analytical calculation of R_0, but also demonstrated the limited value of threshold stability analysis in predicting the evolution of a disease in a dynamic contact network. In future work, this model can be adapted and extended to account for individuals cutting and creating links with knowledge of the state of others in the population, i.e., link-type-dependent network dynamics. This two-way feedback will lead to more sophisticated network properties, such as degree correlations, high clustering, or even network fragmentation. In such cases ODE models need to be used with care, making sure that the agreement with simulations remains valid. Besides modeling epidemics, this framework could also be used to study the spread of information, beliefs, and new ideas within populations, and as such could have implications across a wide range of disciplines beyond the mathematical biology and physics communities.

ACKNOWLEDGMENTS

M.T. acknowledges support from EPSRC (DTA grant). T.J.T. acknowledges support from MRC and the University of Sussex.

[1] R. Albert and A. L. Barabási, Rev. Mod. Phys. **74**, 47 (2002).
[2] M. E. J. Newman, SIAM Rev. **45**, 167 (2003).
[3] M. E. J. Newman, Phys. Rev. E **66**, 016128 (2002).
[4] T. Gross and B. Blasius, J. R. Soc. Interface **5**, 259 (2008).
[5] S. H. Strogatz, Nature (London) **410**, 268 (2001).
[6] S. Bansal, B. T. Grenfell, and L. A. Meyers, J. R. Soc. Interface **4**, 879 (2007).
[7] T. D. Eames and M. J. Keeling, Proc Natl Acad. Sci. USA **99**, 13339 (2002).
[8] H. Anderson, Math. Sci. **24**, 128 (1999).
[9] P. Trapman, Theor. Popul. Biol. **71**, 160 (2007).
[10] L. A. Meyers *et al.*, J. Thoer. Biol. **232**, 71 (2005).
[11] J. M. Read, K. T. D. Eames, and W. J. Edmunds, J. R. Soc. Interface **5**(26), 1001 (2008).
[12] F. Liljeros *et al.*, Nature (London) **411**, 907 (2001).
[13] E. Volz and L. A. Meyers, Proc. R. Soc. B **274**, 2925 (2007).
[14] E. Volz and L. A. Meyers, J. R. Soc. Interface **6**, 233 (2009).
[15] T. Gross, C. J. D. D'Lima, and B. Blasius, Phys. Rev. Lett. **96**, 208701 (2006).
[16] S. van Segbroeck, F. C. Santos, and J. M. Pacheco, PLoS Comp. Biol. **6**, e1000895 (2010).
[17] V. Marceau, P. A. Noel, L. Hebert-Dufresne, A. Allard, and L. J. Dube, Phys. Rev. E **82**, 036116 (2010).
[18] D. H. Zanette and S. Risau-Gusmán, J. Biol Phys. **34**, 135 (2008).
[19] P. Grindrod and D. J. Higham, Proc. R. Soc. A **466**, 753 (2010).
[20] Y. Schwarzkopf, A. Rákos, and D. Mukamel, Phys. Rev. E **82**, 036112 (2010).
[21] N. Low *et al.*, Int. J. Epidemiol. **38**(2), 435 (2009).
[22] J. Lindquist *et al.*, J. Math Biol. **62**, 143 (2010).
[23] J. P. Gleeson, Phys. Rev. Lett. **107**, 068701 (2011).
[24] M. J. Keeling and K. T. D. Eames, J. R. Soc. Interface **2**, 295 (2005).
[25] O. Diekmann and J. A. P. Heesterbeek (Cambridge University Press, 2000).
[26] J. Li, D. Blakeley, and R. Smith, Comp. Math. Meth. Med. doi:10.1155/2011/527610 (2011).